Fine-Grained Local Dynamic Load Balancing in PDES

Jonatan Lindén
Dept. of Information Technology
Uppsala University, Sweden
jonatan.linden@it.uu.se

Pavol Bauer
Dept. of Information Technology
Uppsala University, Sweden
pavol.bauer@it.uu.se

Stefan Engblom
Dept. of Information Technology
Uppsala University, Sweden
stefane@it.uu.se

Bengt Jonsson
Dept. of Information Technology
Uppsala University, Sweden
bengt@it.uu.se

ABSTRACT

We present a fine-grained load migration protocol intended for parallel discrete event simulation (PDES) of spatially extended models. Typical models have domains that are fine-grained discretizations of some volume, e.g., a cell, using an irregular three-dimensional mesh, where most events span several voxels. Phenomena of interest in, e.g., cellular biology, are often non-homogeneous and migrate over the simulated domain, making load balancing a crucial part of a successful PDES. Our load migration protocol is local in the sense that it involves only those processors that exchange workload, and does not affect the running parallel simulation. We present a detailed description of the protocol and a thorough proof for its correctness. We combine our protocol with a strategy for deciding when and what load to migrate, which optimizes both for load balancing and inter-processor communication using tunable parameters. Our evaluation shows that the overhead of the load migration protocol is negligible, and that it significantly reduces the number of rollbacks caused by load imbalance. On the other hand, the implementation mechanisms that we added to support fine-grained load balancing incur a significant cost.

KEYWORDS

Parallel Discrete-Event Simulation; PDES; Load Balancing; Load Migration; Load Metric

ACM Reference Format:
Jonatan Lindén, Pavol Bauer, Stefan Engblom, and Bengt Jonsson. 2018. Fine-Grained Local Dynamic Load Balancing in PDES. In *Proceedings of SIGSIM Principles of Advanced Discrete Simulation (SIGSIM-PADS'18).* ACM, New York, NY, USA, 12 pages. https://doi.org/10.1145/3200921.3200928

1 INTRODUCTION

Discrete Event Simulation (DES) is an important tool in a wide-ranging area of applications, such as integrated circuit design, systems biology, epidemics, etc. To improve performance and accommodate for large scale models, a vast repertoire of techniques have been developed for Parallel DES (PDES) during the last 30 years [15, 20, 25]. New synchronization techniques have been triggered by the advent of multicore processors (e.g., [6, 26, 31]). Still, achieving good performance and speedup for larger numbers of processing elements has proven to be very difficult in the general case.

In PDES, the simulation model is partitioned onto logical processes (LPs), each of which processes timestamped events to evolve its partition along a local simulation time axis. Events that affect the state of neighboring LPs are exchanged to incorporate inter-LP dependencies. A number of synchronization techniques have been developed in order to guarantee that causally dependent events are processed in the right order, ranging from conservative [25] to optimistic [20] approaches, with many intermediate design choices (see, e.g., the surveys [8, 19]). Such intermediate protocols can reduce the performance loss caused by temporary variations in relative speed of different LPs. However, perhaps the most important prerequisite for high efficiency in PDES is that the simulation load is evenly partitioned over LPs This follows from the observation that the total simulation speed can never exceed that of the slowest LP (assuming a one-to-one correspondence between LPs and processors). For simulation models where the distribution of work does not vary over time, this can be achieved by a good static partitioning of the model before simulation starts. However, in many simulation models, the distribution of work varies with time. For instance, in systems biology, the phenomena of interest are often non-homogeneous and migrate over the simulation domain; examples include nerve signals, and the oscillation of proteins involved in the cell division of bacteria [14]. For such models, good parallel performance requires a dynamic load balancing mechanism, which detects when load imbalances arise and corrects them by migrating load between LPs.

Most existing approaches perform dynamic load balancing as a globally coordinated operation, at specified (often regular) time intervals [3–5, 12, 18, 23, 27–29, 32]. For models, where the load migrates continuously over the domain of the simulation model, load imbalances arise locally, and it seems more natural to let rebalancing be a local operation, which involves only those LPs that are affected by the migrating load, and is performed on-line. Such a mechanism must be designed carefully to preserve correctness of the underlying simulation.

SIGSIM-PADS'18, May 23–25, 2018, Rome, Italy

ACM ISBN 978-1-4503-5092-1/18/05…$15.00
https://doi.org/10.1145/3200921.3200928

In this paper, we present an online fine-grained dynamic load migration protocol, which is local in the sense that it concerns only those LPs that are affected by the migrated load. Our protocol is defined for simulation of spatial models that are discretized into *subvolumes* (also known as voxels) which are partitioned onto LPs. An example model is a bacterial cell, where the state of each voxel is represented by a number of entities of different proteins. Each LP is mapped to a core in a multicore processor. Our protocol migrates individual voxels between LPs, with low overhead for the underlying simulation algorithm. It assumes no restrictions on the topology of the simulation domain, nor on the number of LPs adjacent to a migrated element.

Our underlying implementation uses the time-warp protocol [20], with some optimizations. One of these is the use of *aggregated anti-messages*, each representing a set of inter-core anti-messages, that reduce inter-core communication to improve performance. These require extra care in the migration protocol, since their semantics may change as a result of voxel migration. We have therefore developed a proof of correctness of our time-warp protocol with voxel migration. The proof is inspired by that of [22], but adapted to our version of time-warp with aggregated anti-messages, and thereafter extended to cover the migration protocol.

A load balancing mechanism must also include a load metric which represents the amount of load on an LP, and a mechanism for deciding which voxels to migrate where. Defining a good load metric in optimistic PDES is challenging, since natural metrics such as the average CPU load, are no good indicators of the actual simulation progress, since CPUs may be busy processing rollbacks. Many existing approaches [1, 10, 12, 27] to load balancing in PDES base their load migration choices on an LPs load metric related to some global computation including all LPs' load metrics. As our load migration protocol is local, there is a need for a local load metric. Here, our starting point is that observed synchronization costs, such as rollback processing, are very likely caused by load imbalance. In the ideal case, when the load is perfectly balanced, (almost) no messages arrive too late, and thus there should be no need for rollbacks. We therefore use the number of locally incurred rollbacks as a load metric. Even though it is not realistic to completely avoid rollbacks, it is reasonable to assume that by continuous dynamic rebalancing of the load, their incurred overhead should be substantially lower than the overhead of adding an optimism control protocol: our simulator therefore does not employ any additional optimism control.

We show the correctness of the load balancing protocol, and evaluate the performance of our approach, together with two simple metrics for when and where load balancing is needed, on realistic benchmarks from computational cellular biology. Our evaluation shows that the overhead of the load migration protocol is negligible and that it significantly reduces the number of rollbacks caused by load imbalance. On the other hand, the implementation mechanisms that we added to support fine-grained load balancing incur a significant cost.

The paper is organized as follows. In the next section, we give an overview of related work. In Section 3, some necessary background and the main ideas of our load migration protocol is presented. In Section 4, a detailed description of the load migration protocol is given. In Section 5, we provide a correctness argument for the migration protocol. In Section 6, we give a short outline of the load metric and load balancing algorithm that we've used for the evaluation of the migration protocol, in Section 7.

2 RELATED WORK

We review related work that addresses three aspects of the load balancing problem: protocols for load migration, load metrics, and finally how load balancing is initiated.

Load Migration Protocols. Different works have considered different granularity of the transferred load of a migration. Deelman and Szymanski [10] consider a dynamic load balancing mechanism on a two-dimensional circular model. The model is partitioned into segments, each assigned to an LP. Thus, this is a rather simple topology, where each LP only has two neighbors. The load balancing mechanism moves entire columns of the simulated domain between adjacent processing elements. Similarly Schlagenhaft et al. [30] move clusters of basic elements between processing elements. However, they discard the option of moving single elements between partition, which we have opted for in this paper. They argue that no significant change in load balance is achieved when moving small basic elements between processors, but do not further investigate how the granularity of the migrations affects performance. We argue that load imbalance is a local phenomenon, thus accordingly migrations have to be fine-grained.

Load balancing through process migration is studied in Glazer and Tropper [18], Reiher and Jefferson [28] (and in [29], but there process migration was only mimicked). It requires operating system support, and with large numbers of migration units the overhead becomes substantial.

Load balancing for conservative simulation in a shared-memory environment is addressed by Gan et al. [16]. In their dynamic partitioning scheme, LPs are shared through a central pool. To use their method, it has to be decided when an LP should be put back into the pool and simulation should continue at another LP, e.g., when an LP is blocked in conservative simulation. The same decision is non-trivial in optimistic PDES.

A few works outline their load migration protocol, albeit very concisely [1, 4]. We give a detailed description of the load migration protocol and a correctness proof.

Load Metrics. Many proposed load metrics relate to either the local virtual time of each LP in relation to wall-clock time [12, 18, 27, 29, 30] or in relation to the GVT [23], in some cases also related to the number of processed or committed (i.e., with timestamp smaller than GVT) events [23, 27]. Deelman and Szymanski [10] use the number of future scheduled events, weighted by imminence. Instead, we look at the number of incurred rollbacks, which to the best of our knowledge has not been evaluated before.

In comparison to load balancing procedures of other aggregated LP approaches such as [1, 10, 30] (and to some extent [27]), our load metric is local to each basic element of computation, and not aggregated per cluster/LP (depending on notation used).

Some works have taken the communication cost between LPs in account [1, 10, 27]. In [27], a load metric and a communication metric is used alternately during migration. In [10], the communication cost of a migration is handled implicitly by only allowing

whole columns of the 2-dimensional simulation state to be migrated. In [1], the migration candidate (with high load metric) with the smallest communication metric is selected. Our method is similar to that in [1], but it is local (i.e., the migration candidates come from a small region).

Initiation of Load Balancing. Many papers on load balancing in PDES prescribe that the load balancing should be initiated at regular time periods, ranging from less than 5 seconds of wall-clock time to 10 minutes of simulation time [3, 5, 18, 23, 27–29, 32, 33], sometimes also expressed in multiples of GVT computations [4, 12]. The optimal period depends on the model and the speed of the computer on which the simulator is running. In our method, load balancing is initiated by a high rollback rate, thus it is independent of the computer speed and dependent on the model to a lower degree.

Some papers have looked into a more dynamic approach to initiation of load balancing. In [1], a non-static interval is used, based on measurements taken every 3 seconds. In [7], a non-static interval is used, based on data updated every 500 events received. In [30] and [1], the authors try to account for the temporary performance decrease a load migration incur. In [1], a migration is initiated first when the integral of the actual throughput of the simulator, using migrations, is superior to the integral of a projected estimated throughput, had no load balancing taken place.

3 FRAMEWORK

Our load balancing protocol is developed in the context of spatial stochastic simulation. Since this context has influenced some of our design decisions, we describe it here briefly.

3.1 Spatial Stochastic Simulation

The reaction-diffusion master equation (RDME) [17] describes systems where entities diffuse in some volume and may undergo transitions, or reactions, when in proximity to each other. The RDME is a popular tool for modeling biological systems where the population of entities is low and discrete effects therefore play an important role for the behavior of the systems.

In the context of RDME, simulation models are defined over a spatial domain, which is discretized into *subvolumes*, also known as *voxels*. Each voxel contains a discrete *copy number* of entities of some set of species (e.g., proteins). The dynamics of the model is described by a spatially extended Markov process, in which two types of transitions are possible: (i) in a *reaction* a combination of species residing in a voxel reacts and produces a new combination within the same voxel, (ii) in a *diffusion* a single entity of a species moves to a neighboring voxel. In general, each voxel can host several types of reactions with different combinations of entities. The inter-event times between reactions and diffusions are stochastic, highly variable and without a lower bound. An important feature of typical models is that diffusions are significantly more common than reactions (by at least a factor of 10), and that the local state of each voxel is relatively simple (consisting of the copy numbers of all participating species).

Practically, the RDME is simulated using sampling methods that produce single trajectories from the relevant probability space. The most commonly used such method is the Next Subvolume Method (NSM) [13]. The NSM algorithm takes the form of DES, whose event queue contains the next occurrence time of the next event within each voxel. The execution of that voxel event first decides (by a random draw) which particular reaction or diffusion will occur, and then performs it: the the states of concerned voxels are updated, and the voxel's next occurrence time is inserted into the event queue.

3.2 Parallelization using Standard Time Warp

Since the number of voxels is typically large, the natural approach to parallelization is to partition the set of voxels into subdomains, each of which is assigned to an LP, which is then mapped to a processing element. Each LP simulates the dynamics of its subdomain, using the NSM algorithm. We use the Time Warp synchronization mechanism [20] without optimism control. In order to support migration of voxels between LPs, voxel-specific information is stored in a self-contained structure, which for each voxel v maintains

- v.state, the local state of v,
- v.next, the time of its next event occurrence,
- v.history, the history of its processed events,
- v.routing, a routing table maps each voxel neighbor in the simulation model to the index of the LP on it is located.

We let LVT(v) be the time of the most recent event in v.history; intuitively, this is the local simulation time of voxel v. Each LP LP_i itself maintains LP-global information, viz.

- $\mathrm{LP}_i.EventQueue$, a time-sorted event queue, containing the occurrence time of the next event of each voxel in its subdomain,
- $\mathrm{LP}_i.bnd$, which maps each neighboring LP LP_j of LP_i to the set of voxels of LP_i that have some neighbor on LP_j. This is used to define the meaning of aggregated anti-messages (defined below), i.e., voxels in $\mathrm{LP}_i.bnd(\mathrm{LP}_j)$ will be rolled back when an aggregated anti-message is received from LP_j.

Each pair of neighboring LPs exchange messages via unidirectional channels. We let $chan_{i\to j}$ denote the channel from $\mathrm{LP_i}$ to $\mathrm{LP_j}$ (there is then also a channel $chan_{j\to i}$ in the opposite direction). Each diffusion to a voxel residing on a different LP induces a message to that LP. We use $v \xrightarrow{t} v'$ to represent a message denoting that a diffusion from voxel v to voxel v' has occurred at time t (the message also contains the diffused species, which we ignore here). Channels also carry other types of messages: anti-messages, and control messages associated with the migration protocol, which are described later.

Each LP advances the simulation by finding the next event to process, either from the top of its event queue or from a message that is at the front of an incoming channel. Thereafter, the event is processed by (1) updating the states of affected voxels, (2) adding the event to the histories of affected voxels, and (3) if the event was taken from the event queue, determining a new next event time for the initiating voxel. If the event is a diffusion to another LP, a diffusion message is transmitted to the neighbor.

Selective Rollback. Whenever the next event to process is an incoming diffusion message of form $v \xrightarrow{t} v'$ such that $t \le \mathrm{LVT}(v')$ (also called a *straggler*), a rollback is initiated. To do so, events are processed "backwards" until such a previous time is reached. A simple approach would be to roll back all events performed by the LP of v' with a time stamp higher than t. However, it is

typically less costly to perform a *selective rollback*, which only rolls back events that may be causally dependent on rolled back events involving v' [2, 9]. In addition, rollback of causally dependent events performed on other LPs must be initiated by sending anti-messages to concerned LPs. In our algorithm, anti-messages are aggregated per LP, i.e., in each rollback, at most one anti-message is sent per neighboring LP. An aggregated anti-message from LP_i to LP_j only carries a single timestamp, which is the minimum timestamp of a rolled back inter-LP diffusion at LP_i which also involves LP_j. Since the anti-message is only a single timestamp, it will initiate rollback of all inter-LP diffusions involving both LP_i and LP_j, even those that are not causally dependent on the initiating straggler.

More precisely, the rollback procedure on an LP_i can be described by specifying for each voxel v of LP_i a rollback time $RBT(v)$, and for each neighbor LP_j of LP_i, a time $AMT(\mathrm{LP}_j)$ for its anti-message. These times are the largest ones (including ∞) that satisfy the following constraints:

(1) if a straggler $v \xrightarrow{t} v'$ arrives to LP_i, then $RBT(v') < t$,
(2) if voxels v and v' of LP_i have performed a joint diffusion at time t with $RBT(v) \leq t$, then $RBT(v') \leq t$,
(3) if voxel v of LP_i has performed a diffusion $v \xrightarrow{t} v'$ such that $v' \in \mathrm{LP}_j$ and $RBT(v) \leq t$, then $AMT(\mathrm{LP}_j) \leq t$,
(4) if voxel v of LP_i has performed a diffusion $v \xrightarrow{t} v'$ such that $v' \in \mathrm{LP}_j$ and $AMT(\mathrm{LP}_j) \leq t$, then $RBT(v) \leq t$.

Intuitively, Conditions 1 and 2 describe the causality constraints for rolling back voxels on LP_i, Condition 3 specifies the timestamp of the aggregated anti-message to LP_j, and Condition 4 specifies the additional rollback that is caused by assuming that the anti-message represents all diffusions between LP_i and LP_j that are not earlier than $AMT(\mathrm{LP}_j)$.

When an aggregated anti-message from LP_j with time t arrives to LP_i, then a rollback is initiated with the same constraints as above, except that condition 1 is replaced by

(1') if voxel v of LP_i has received a diffusion $v' \xrightarrow{t'} v$, with $v' \in \mathrm{LP}_j$ and $t \leq t'$, then $RBT(v) < t'$.

4 MIGRATION ALGORITHM

In this section, we describe in detail the essential algorithms involved in the migration protocol. We start by describing the data structures being used, thereafter we describe the rollback and anti-message routines, and finally we describe the processing of messages and the core migration protocol.

4.1 Migration of a Voxel

A voxel v is migrated between two LPs by sending a control message $\overrightarrow{v}$ containing v. In the implementation, what is actually sent is a pointer to the structure representing v, which includes v.history, v.routing and v.next. Both the sending and the receiving LP will update relevant status information concerning v upon sending and receiving this message. The main challenge is that any messages being in flight to the migrated voxel v have to be rerouted, and must be guaranteed to arrive in the correct order. That is, to ensure correctness, it must be guaranteed that for any pair of voxels v_0, v_1, messages sent from v_0 to v_1, including anti-messages, are received in the same order as they are sent. A particular challenge is that anti-messages are aggregated, and that their meaning changes as a result of the migration. The protocol must therefore be carefully designed to consider also this complication.

In Algorithm 1 the procedure for sending a voxel v from $\mathrm{LP}_{\mathrm{src}}$ to $\mathrm{LP}_{\mathrm{dst}}$ is described. At line 2, the Lock function ensures that no voxel neighbor to v is migrated simultaneously with v, details are described in Algorithm 3. Essentially, it atomically sets a *migration flag* on the channel to each neighboring LP that maintains a voxel neighbor to v. If one such flag already is set, i.e., the migration of some voxel neighbor v' to v has already been initiated, then the migration of v is aborted. At lines 3 and 4, v is removed from the local state. At line 6 internal routing information of v's neighboring voxels are updated to locate v on $\mathrm{LP}_{\mathrm{dst}}$. At line 7 the boundary list of voxels bordering $\mathrm{LP}_{\mathrm{dst}}$ is updated to contain all neighboring voxels of v. The function returns a set of neighbors Neigh on which v had neighbors. Since the neighbors in Neigh has voxels who are neighbors to v, these neighbors have to be informed about the migration, by means of message sent at line 10. The actual voxel is sent to $\mathrm{LP}_{\mathrm{dst}}$ at line 11.

Algorithm 1 Sending a voxel v from $\mathrm{LP}_{\mathrm{src}}$ to some $\mathrm{LP}_{\mathrm{dst}}$.

```
1  function SendVoxel(v)
2    if Lock(v) then return
3    EventQueue ← {⟨v_k, t⟩ | ⟨v_k, t⟩ ∈ EventQueue ∧ v_k ≠ v}
4    State ← State \ v
5    for each v_nbr ∈ LP_src that is a neighbor to v do
6      v_nbr.routing[v] ← LP_dst
7      bnd(LP_dst) ← bnd(LP_dst) ∪ v_nbr
8    for each LP_k ≠ LP_src with a neighbor to v do
9      remove v from bnd(LP_k)
10     Send(mv_v(LP_dst), LP_k)
11   Send(v⃗, LP_dst)
```

Our protocol for migrating a voxel v_m from $\mathrm{LP}_{\mathrm{src}}$ to $\mathrm{LP}_{\mathrm{dst}}$ makes use of the following control messages.

$\overrightarrow{v_m}$ is a control message, which transfers the migrated voxel v_m,

$\mathrm{mv}_{v_m}(\mathrm{LP}_{\mathrm{dst}})$ is sent by $\mathrm{LP}_{\mathrm{src}}$ to each LP (except $\mathrm{LP}_{\mathrm{dst}}$) whose domain contains neighbors of v_m, announcing that the voxel v_m has just been sent to $\mathrm{LP}_{\mathrm{dst}}$,

recv_{v_m} is sent by $\mathrm{LP}_{\mathrm{dst}}$ to each LP (except $\mathrm{LP}_{\mathrm{src}}$) whose domain contains neighbors of v_m, announcing that the voxel v_m has just been received at $\mathrm{LP}_{\mathrm{dst}}$,

forw_{v_m} is sent to $\mathrm{LP}_{\mathrm{dst}}$ by each LP (except $\mathrm{LP}_{\mathrm{src}}$) whose domain contains neighbors of v_m, announcing that they has received recv_{v_m} and is about to send normal messages (containing diffusion events) to v_m.

An overall description of the message protocol for migrating a voxel v_m follows.

- $\mathrm{LP}_{\mathrm{src}}$ initiates the migration by sending $\overrightarrow{v_m}$ to $\mathrm{LP}_{\mathrm{dst}}$. At the same time, $\mathrm{LP}_{\mathrm{src}}$ also sends the message mv_{v_m} to each neighbor LP_k (except $\mathrm{LP}_{\mathrm{dst}}$) whose domain contains some voxel neighbor of v_m, announcing that the voxel v_m has just been sent to $\mathrm{LP}_{\mathrm{dst}}$. For each such neighbor LP_k, and also for $\mathrm{LP}_{\mathrm{dst}}$, $\mathrm{LP}_{\mathrm{src}}$ creates a temporary data structure, denoted $log_{k\to\mathrm{src}}(v_m)$, in which it stores all received messages and anti-messages to v_m; these messages will thereafter be retrieved by LP_k in order to forward them to $\mathrm{LP}_{\mathrm{dst}}$.

- upon receipt of mv_{v_m}, each LP_k (except LP_{src} and LP_{dst}) which formerly sent messages to v_m via $chan_{k\to\text{src}}$, will first send the message forw_{v_m} to LP_{dst}, announcing that it will start to send messages to v_m over $chan_{k\to\text{dst}}$. Thereafter, it retrieves all such messages sent, but not yet received, from $log_{k\to\text{src}}(v_m)$ and $chan_{k\to\text{src}}$, and thereafter forwards them (in order) to LP_{dst} (over $chan_{k\to\text{dst}}$).
- Upon receipt of $\overrightarrow{v_m}$, LP_{dst} sends a message recv_{v_m} to LPs (except LP_{src}) whose domain contains neighbors of v_m, announcing that the voxel v_m has been received at LP_{dst}. Thereafter, it will (in the same manner as LP_k in the previous step) retrieve all messages to v_m sent, but not yet received, from $log_{\text{dst}\to\text{src}}(v_m)$ and $chan_{\text{dst}\to\text{src}}$. The events in these messages are then rolled back.

The control messages recv_{v_m} and forw_{v_m} block, i.e., prevent any message from being received, from the channels from which they were retrieved, unless $\text{mv}_{v_m} < \text{recv}_{v_m}$ and $\overrightarrow{v_m} < \text{forw}_{v_m}$, respectively (where $<$ denotes order of reception).

In Algorithm 2, the detailed protocol logic for how an LP handles the different types of incoming messages is described. For each message type, the description refers to lines in Algorithm 2, unless stated otherwise. In the algorithm, the LP where a message is received is denoted LP_i, and the sending LP is denoted LP_k.

$\overrightarrow{v}$ The message $\overrightarrow{v}$ carries a migrating voxel v. Upon receipt of $\overrightarrow{v}$, LP_i first updates its bookkeeping information: v is added to the local state (lines 3 and 4), the routing tables of v's neighboring voxels are updated (lines 5 to 8), v is marked as located on LP_i in each neighbouring voxel's internal routing table (line 6), and v's local neighbors are also removed from the list of voxels bordering LP_k, if they no longer have any neighbours on LP_k (line 8). Thereafter, a message recv_v is sent to each LP (other than LP_k) with a neighbor voxel of v, informing that the migration has completed (line 11). If any incoming channel is closed due to the migration of v (i.e., a message forw_v has been received from some LP_j), it can now be reopened (line 12). Thereafter, LP_i retrieves all pending messages sent from LP_i to v, from the temporary structure $log_{i\to k}(v)$ stored at LP_k and from $chan_{i\to k}$; this retrieval also transforms aggregated anti-messages (with only a time t) into voxel-specific anti-messages (denoted $-t_v$). The retrieval from the channel is performed in the function Project, described by (1) below. The sequence of retrieved messages are collected into the ordered list M_v (line 13). The projected diffusions are simultaneously removed from the corresponding channel, and the migration flag for v in $chan_{i\to k}$ is unset, indicating that no more messages should be added to the backlog $log_{i\to k}(v)$ when messages are received from $chan_{i\to k}$ (lines 15 and 16). Finally, the state of v and the messages in M_v are rolled back (lines 17 to 20), to avoid any ordering conflicts of future and already sent messages.

$\text{mv}_v(\text{LP}_j)$ This type of message is sent to LPs that have voxel neighbors to some migrating voxel $\overrightarrow{v}$ destined for LP_j, but which are not the recipient of $\overrightarrow{v}$ (at line 10 in Algorithm 1). Upon the receipt of the message at some LP_i, retrieves into M_v all pending messages sent from LP_i to v, from the temporary structure $logik(v)$ stored at LP_k and from $chan_{i\to k}$ in the same way as described for messages of type $\overrightarrow{v}$ (using the function Project). The messages in M_v are forwarded to LP_j, the new LP of v, in the same order they previously were sent to LP_k, prefixed by a message of type forw_v (lines 26 and 27). Thereafter, for each voxel-neighbor v_n to v residing on LP_i, the LPs boundary information is updated as follows: If v_n has no other voxel neighbors on LP_k, then v_n is removed from the list of voxels representing the boundary to LP_k (line 31). The set of v's voxel neighbors is then stored in *mvbnd*, tagged with v (line 32). The voxels will later be added to the boundary of LP_k facing LP_j. If the channel from LP_j to LP_i is marked as closed, then it is reopened, and each voxel-neighbor v_n are immediately added to the list of voxels bordering to LP_j (lines 33 to 36).

recv_v This type of message is sent by the LP receiving a message $\overrightarrow{v}$ to LPs that are not the sender of the message $\overrightarrow{v}$, but have voxels neighboring v. Upon receipt of a message recv_v at LP_i, a check is done whether a corresponding message mv_v has been received, by checking if tag v exists in the set *mvbnd* (line 38). If not, the channel to LP_i is closed to enforce that a message mv_v is received first for each migration of a voxel. Otherwise, the set of v's neighboring voxels on LP_k, previously bordering LP_i, are now included in the boundary towards LP_j (line 41).

forw_v This type of message is sent by an LP that has voxels neighboring some recently migrated voxel v, but was neither the sender nor the recipient of the corresponding migration message $\overrightarrow{v}$. It is sent to the LP to which v has been migrated. The message indicates that after the transmission of forw_v from LP_k to LP_j, LP_k starts forwarding messages destined for v to LP_j. Upon receipt of forw_w, LP_j checks if $\overrightarrow{v}$ has already been received. If not, the channel $chan_{k\to j}$ is closed (line 50). This enforces that $\overrightarrow{v}$ is received before any messages destined for v.

$-t$ When receiving an anti-message $-t$ from LP_k at time t, the history of each voxel v that may have received a diffusion from LP_k is scanned (line 43). If there is such a diffusion $w \xrightarrow{t'} v, w \in \text{LP}_k$ which happened after t, rollback v_i to t' (line 44). Then, for all voxels that have been migrated to some other LP, say LP_j, and who previously were on the boundary to LP_k (and thus have an entry in $chan_{k\to i}$.flags), a copy of the anti-message is put in the corresponding backlog (line 45).

$w \xrightarrow{t} v$ When receiving a diffusion, if the receiving voxel v has migrated, the diffusion is added to the backlog of messages for v, located on $chan_{k\to i}$ (line 53). If the diffusion is a straggler, a rollback is performed (line 55), before processing the diffusion (line 56).

The Project function (1) extracts all messages in a channel *chan* destined for a voxel v. It should be noted, that the channel is protected by a lock, thus the effect of Project is observed to take place instantaneously for any LP. The projection is done as follows: The messages in *chan* are recursively traversed. Diffusions destined for v are returned, and anti-messages $-t$ are converted to local anti-messages $-t_v$, only affecting v. Other messages are

Algorithm 2 Receipt of message from LP_k at LP_i.

```
1  function HandleMessage(m)
2    if m = v⃗ then
3      EventQueue ← insert (EventQueue, ⟨v.next, v⟩)
4      State ← State ∪ v
5      for each v_nbr ∈ LP_i that is a neighbor to v do
6        v_nbr.routing[v] ← LP_i
7        if v_nbr has no more neighbors on LP_k then
8          remove v_nbr from bnd(LP_k)
9      add v to bnd(LP_k)
10     for each LP_j ≠ LP_k with a neighbor to v do
11       Send(recv_v, LP_j)
12       if chan_{j→i} closed by migration of v then open chan_{j→i}
13     M_v ← log_{i→k}(v)+Project(chan_{i→k}, v)
14     log_{i→k}(v) ← ∅
15     remove all diffusions destined for v from chan_{i→k}
16     remove ⟨v, LP_k⟩ from chan_{i→k}.flags
17     t_min ← min{ t | w -t→ v ∈ M_v ∨ −t ∈ M_v ∨ −t_v ∈ M_v }
18     Rollback(v, t_min)
19     for each w -t→ v ∈ M_v do
20       Rollback(w, t)
21   if m = mv_v(LP_j) then
22     M_v ← log_{i→k}(v)+Project(chan_{i→k}, v)
23     log_{i→k}(v) ← ∅
24     remove all diffusions destined for v from chan_{i→k}
25     remove ⟨v, LP_k⟩ from chan_{i→k}.flags
26     Send(forw_v, LP_j)
27     Send(M_v, LP_j)
28     V_bnd ← {v_nbr | v_nbr ∈ LP_i ∧ v_nbr neighbor to v}
29     for each v_nbr ∈ V_bnd do
30       if v_nbr has no more neighbors on LP_k then
31         remove v_nbr from bnd(LP_k)
32     mvbnd ← mvbnd ∪ ⟨v, V_bnd⟩
33     if chan_{j→i}.closed then
34       bnd(LP_j) ← bnd(LP_j) ∪ V_bnd s.t. ⟨v, V_bnd⟩ ∈ mvbnd
35       if chan_{j→i} closed by migration of v then
36         open chan_{j→i}
37   if m = recv_v then
38     if ∄ V_bnd.⟨v, V_bnd⟩ ∈ mvbnd then
39       close channel chan_{k→i}
40     else
41       bnd(LP_k) ← bnd(LP_k) ∪ V_bnd s.t.⟨v, V_bnd⟩ ∈ mvbnd
42   if m = −t then                ▷ Aggregated anti-message
43     for each v ∈ bnd(LP_k) do
44       Rollback(v, t)            ▷ According to (1'), Section 3
45     for each ⟨v, LP_j⟩ ∈ chan_{k→i}.flags do
46       log_{j→i}(v) ← log_{j→i}(v) · −t_v
47   if m = −t_v then              ▷ Local anti-message
48     Rollback(v, t)              ▷ According to (1'), Section 3
49   if type = forw_v then
50     if v ∉ State then close chan_{k→i}
51   if m = w -t→ v then           ▷ Regular diffusion to v
52     if v ∉ State then           ▷ v is migrated to some other LP
53       log_{k→i}(v) ← log_{k→i}(v) · m
54     if t ≤ LVT(v) then          ▷ Handle straggler
55       Rollback(v, t)
56     process w -t→ v
```

filtered out.

$$\textsc{Project}(chan, v) = \begin{cases} m \cdot \textsc{Project}(chan, v) & \text{if } m = w \xrightarrow{t} v \\ -t_v \cdot \textsc{Project}(chan, v) & \text{if } m = -t \\ \textsc{Project}(chan, v) & \text{otherwise} \end{cases} \quad (1)$$

In Algorithm 3, we see the mechanism for preventing simultaneous migrations of neighboring voxels. For all channels coming from LPs where v has a neighbor, a migration flag is set marking that an attempt migrating v is undertaken (line 5). If, after having set the flag, a flag of the corresponding neighbor is seen on the outgoing channel, all flags already set on the channels are unset, and the lock procedure returns false (line 8). If the procedure manages to set all flags without seeing a flag set on a corresponding outgoing channel, it has succeeded the migration may take place, and returns true.

Algorithm 3 Prevent simultaneous migration of a voxel v from LP_i and any of its neighbors v_n.

```
1  function Lock(v)
2    V_n ← {v_n | v_n ∉ LP_i ∧ v_n neighbor to v}
3    for each v_n ∈ V_n do
4      m ← v.routing[v_n]
5      chan_{m→i}.flags ← chan_{m→i}.flags ∪ v
6      if v_n ∈ chan_{i→m}.flags then
7        unset all set flags and abort
8        return false
9    return true
```

p

5 CORRECTNESS

In this section, we give a proof for the correctness of our migration protocol. It is inspired by that of [22], but adapted to cover our version of time-warp with aggregated anti-messages and voxel migration. We will focus on the property of safety: that any parallel execution produces the same simulation run as the corresponding sequential simulation algorithm. The notion of "produced simulation run" is well-defined if the simulation model is deterministic, so that a simulation run is uniquely determined by the initial state and the transition rules, which in our case are fixed (we make the assumption that no two events in a voxel have exactly the same time-stamp). In the presence of random events, the simulation is made deterministic by using deterministic pseudorandom number generators, whose states are included in the local states of the corresponding voxels, and which are reverted together with the voxel state when performing rollbacks.

As described in Section 3, our simulation models consist of voxels, which evolve the state of the model by performing reactions, which are local, and diffusions that also affect the state of a neighbouring voxel. Within a voxel v, the simulation run is defined by the ordered sequence v.history of its processed time-stamped events. We define $\mathrm{In}^{v'}(v)$ as the sequence of processed incoming diffusion from v' in v.history, and let $\mathrm{Out}^{v'}(v)$ be the sequence of sent diffusions to voxel v' in v.history. A sequential simulation run satisfies the following two properties.

(i) The history v.history in a sequential simulation is the one that is uniquely determined by following the simulation

rules from the initial voxel state and the sequences $\text{In}^{v'}(v)$ of processed incoming diffusion messages from each neighbour v' in the simulation model.

(ii) For each pair v, v' of neigbour voxels in the simulation model, $\text{In}^{v}(v') = \text{Out}^{v'}(v)$, i.e., the sequence of incoming diffusions to v' from v is the same as the sequence of outgoing diffusions from v to v'.

Property (i) uses the assumption that no two events in v.history have exactly the same timestamp. Property (ii) follows by noting that in a sequential simulation, a diffusion from v to v' is simultaneously added both to v.history and to v'.history.

Conversely, any completed simulation run, which is constructed from voxel histories that satisfy (i) and (ii) is the same as the uniquely defined simulation run. We can then establish safety of the parallel simulation by proving that it satisfies properties (i) and (ii).

Property (i) for the parallel simulation algorithm can be established by checking that each step (both forward simulation steps and rollbacks) in the simulation algorithm respect the rules of the simulated model. This is not difficult, an we omit the details.

Property (ii) is less straightforward: in general it does not hold during the simulation run, since diffusion messages and anti-messages may be in transit between v and v' when they reside on different LPs. We will therefore replace property (ii) by a set of invariants that hold during the simulation, and which imply property (ii) when the simulation is completed and channels are empty. In the remainder of this section, we will formulate and prove this set of invariants. In Subsection 5.1 we formulate and prove them for our version of the underlying Time Warp algorithm. Then, in Subsection 5.2, we will extend them to our migration protocol.

Notation. We say a message is of the form $v \to v'$ if it is sent from v and destined for v'. We write a timestamp ordered sequence of messages $m_0 \cdot m_1 \cdots m_n$, where we let m_0 be the oldest message in the sequence, and m_n the most recent. We use $+\!\!+$ to denote concatenation of sequences. We let $\text{In}^{v}(v')$ be the sequence of processed diffusion messages of form $v \to v'$ in v'.history, and let $\text{Out}^{v'}(v)$ be the sequence of sent diffusion messages of form $v \to v'$ in v.history. In particular, no anti-messages occur in the histories. The time of the earliest anti-message affecting a voxel v (aggregated or local), in a channel *chan*, is denoted *chan*.min(v). If there is no such anti-message, *chan*.min(v) is ∞.

5.1 Correctness for Time Warp

Intra-LP Consistency. For all pairs v, v' of voxel, that reside on the same LP, the incoming and outgoing diffusion histories are always consistent.

$$\text{In}^{v}(v') = \text{Out}^{v'}(v). \tag{IV1}$$

Proof sketch of (IV1). Since each LP processes messages in timestamp order, all diffusions from v to v' are added in timestamp order. At each processing of some event with a timestamp t, both $\text{In}^{v}(v')$ and $\text{Out}^{v'}(v)$ will be extended with the same diffusion. A local rollback caused by a straggler or received anti-message will, by rule (2) of the rollback operation, remove all diffusions from both $\text{In}^{v}(v')$ and $\text{Out}^{v'}(v)$ whose timestamps are greater than some common time t, thereby preserving (IV1). □

Inter-LP Consistency. In the case where the two voxels reside on different LPs, messages reside in a channel *chan* connecting the two LPs, before being received. Thus we must characterize the relationship between in- and out-histories at voxels and the messages in the corresponding channels. To this end, we define the *effect* with respect to voxels v and v' of the messages in a sequence *chan*, denoted $\underset{v\to v'}{\text{effect}}(chan)$, as follows.

$$\underset{v\to v'}{\text{effect}}(chan \cdot m) = \begin{cases} \underset{v\to v'}{\text{effect}}(chan) \cdot m & \text{if } m = v \xrightarrow{t} v' \\ \text{rm}_t(\underset{v\to v'}{\text{effect}}(chan)) & \text{if } m = -t \text{ or } m = -t_{v'} \\ \underset{v\to v'}{\text{effect}}(chan) & \text{otherwise} \end{cases} \tag{2}$$

where $\text{rm}_t(chan)$ is obtained by removing all messages with timestamp $\geq t$ from *chan*. Intuitively, $\underset{v\to v'}{\text{effect}}(chan)$ is the subsequence of diffusions from v to v' in *chan* that will not be reverted by a later anti-message in *chan*. This property can be derived from (2) and expressed as the following property of $\underset{v\to v'}{\text{effect}}(chan)$.

$$\underset{v\to v'}{\text{effect}}(m\cdot chan) = \begin{cases} m \cdot \underset{v\to v'}{\text{effect}}(chan) & \text{if } m = v \xrightarrow{t} v' \text{ and} \\ & \quad (\nexists m' \in chan.\exists t' \geq t. \\ & \quad\quad (m' = -t' \text{ or } m' = -t'_{v'})) \\ \underset{v\to v'}{\text{effect}}(chan) & \text{otherwise} \end{cases} \tag{3}$$

Let v and v' be two neighboring voxels on two different LPs, communicating through a channel *chan*, and let $t = chan.\min(v')$. Then the sequences of diffusions from v to v' in the two voxel histories are related by the following invariant.

$$\text{rm}_t(\text{In}^{v}(v')) +\!\!+ \underset{v\to v'}{\text{effect}}(chan) = \text{Out}^{v'}(v) \tag{IV2}$$

Proof sketch of (IV2). We establish the invariant by induction over the length of a simulation run. Initially, $\text{In}^{v}(v')$ and $\text{Out}^{v'}(v)$ and the channel are empty, and the invariant holds trivially. Assume non-empty $\text{In}^{v}(v')$ and $\text{Out}^{v'}(v)$, and a state of the channel *chan* such that Invariant (IV2) holds. We will let $\text{In}'^{v}(v')$, $\text{Out}'^{v'}(v)$, and *chan*′ be their states after the performed action. Let $t = chan.\min(v')$. Line numbers refer to Algorithm 2. We get the following cases depending on the performed action.

- v's LP sends a diffusion m of form $v \xrightarrow{\hat{t}} v'$ to v''s LP.
  Then $\text{In}'^{v}(v') = \text{In}^{v}(v')$, and $\text{Out}'^{v'}(v) = \text{Out}^{v'}(v) \cdot m$, and $chan' = chan \cdot m$. We get
  $\text{Out}'^{v'}(v) = \text{Out}^{v'}(v) \cdot m =$ (by (IV2))
  $\text{rm}_t(\text{In}^{v}(v')) +\!\!+ \text{effect}_{v\to v'}(chan) \cdot m =$ (by (2))
  $\text{rm}_t(\text{In}^{v}(v')) +\!\!+ \text{effect}_{v\to v'}(chan \cdot m) =$
  $\text{rm}_t(\text{In}'^{v}(v')) +\!\!+ \text{effect}_{v\to v'}(chan \cdot m)$.
- v's LP sends an aggregated anti-message $-\hat{t}$ to v''s LP, while reverting diffusions in $\text{Out}^{v'}(v)$ with a timestamp $\geq \hat{t}$, since $v \in \text{LP}_{\text{dst}}.bnd(\text{LP}_{\text{src}})$ (Condition 4 in the the calculation of RBT in the rollback operation in Section 3). Let $t' = \min(t, \hat{t})$. Then $t' = chan'.\min(v')$.
  We have $\text{Out}'^{v'}(v) = \text{rm}_{\hat{t}}(\text{Out}^{v'}(v)) =$ (by (IV2))
  $\text{rm}_{\hat{t}}(\text{rm}_t(\text{In}^{v}(v'))) +\!\!+ \text{rm}_{\hat{t}}(\text{effect}_{v\to v'}(chan)) =$ (by (2))
  $\text{rm}_{t'}(\text{In}^{v}(v')) +\!\!+ \text{effect}_{v\to v'}(chan \cdot -\hat{t}) =$
  $\text{rm}_{t'}(\text{In}'^{v}(v')) +\!\!+ \text{effect}_{v\to v'}(chan')$.
- v''s LP receives a diffusion m of form $v \xrightarrow{\hat{t}} v'$ from v's LP (line 51). Details are analogous and omitted.

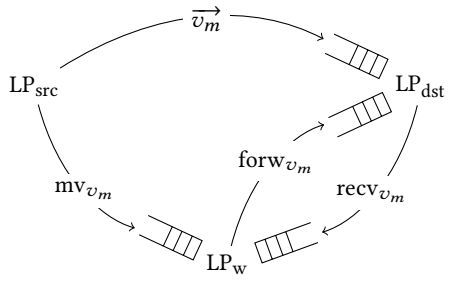

Figure 1: Schematic of LPs involved in the migration of voxel v_m, and the types of messages, $\overrightarrow{v_m}, \text{mv}_{v_m}, \text{recv}_{v_m}$ and forw_{v_m}, being involved in the migration.

- v''s LP receives an anti-message of form $-\hat{t}$ or $-\hat{t}_{v'}$ from v's LP, reverting diffusions in $\text{In}^v(v')$ with a timestamp $\geq \hat{t}$ (lines 42 and 47). Again, details are analogous.

□

5.2 Correctness for the Migration Protocol

In this section, we show that the algorithm maintains consistency when extended with migrations of voxels between two LPs. The migration protocol introduces several types of control messages, viz., $\overrightarrow{v_m}, \text{mv}_{v_m}, \text{recv}_{v_m}$ and forw_m. Since the migration protocol does not modify the histories of voxels directly, effect is defined to ignore such control messages c, i.e., $\text{effect}_{v_\to v'}(chan \cdot c) = \text{effect}_{v_\to v'}(chan)$.

An aggregated anti-message $-t$ changes in meaning when a voxel v_m is migrated from LP_{src} to LP_{dst}. If $-t$ is sent from LP_{src}, after $\overrightarrow{v_m}$, then it does not affect messages sent from v_m to v on LP_{dst}, which is achieved by the removal of v_m from *bnd* in the algorithms (line 9 in Algorithm 1 and line 8 in Algorithm 2). To capture this, we define an operator $\text{cut}_{m'}$, which simply truncates a sequence after the first occurrence of m', by

$$\text{cut}_{m'}(m \cdot chan) = \begin{cases} m & \text{if } m = m' \\ m \cdot \text{cut}_{m'}(chan) & \text{otherwise} \end{cases}$$

5.2.1 Consistency between sender and receiver of migrated voxel. Now, we are ready to define the invariants. Let v_m and v be two neighboring voxels, where v_m, previously located on LP_{src}, is being migrated to the same LP as v, LP_{dst}. We have to show the consistency of messages in both directions relative the migration direction. After the transmission of $\overrightarrow{v_m}$, and before $\overrightarrow{v_m}$ has been received, we have the following two invariants.

- For diffusions from v_m to v:
  Let $t = (\text{cut}_{\overrightarrow{v_m}}(chan_{\text{src}\to\text{dst}}))$. $\min(v)$. Then we have

$$\text{rm}_t(\text{In}^{v_m}(v)) +\!\!+ \underset{v_m \to v}{\text{effect}}(\text{cut}_{\overrightarrow{v_m}}(chan_{\text{src}\to\text{dst}})) = \text{Out}^v(v_m). \tag{IV3}$$

  This invariant is analogous to (IV2), but considers only the part of $chan_{\text{src}\to\text{dst}}$ that precedes $\overrightarrow{v_m}$.

- For diffusions from v to v_m:
  Let $t = (log_{\text{dst}\to\text{src}}(v_m) +\!\!+ chan_{\text{dst}\to\text{src}})$. $\min(v_m)$. Then

$$\text{rm}_t(\text{In}^v(v_m)) +\!\!+ \underset{v \to v_m}{\text{effect}}(log_{\text{dst}\to\text{src}}(v_m) +\!\!+ chan_{\text{dst}\to\text{src}}) = \text{Out}^{v_m}(v). \tag{IV4}$$

  This invariant extends (IV2) by considering that diffusions from v to $\overrightarrow{v_m}$ are collected in $log_{\text{dst}\to\text{src}}(v_m)$.

We note that v_m neither can send nor receive any messages while in transit, thus the proof of Equation (3) is only concerned with v receiving a message, and the proof of Equation (4) is only concerned with v sending a message.

5.2.2 Correctness of receipt of migrated voxel. During migration of a voxel v_m, consistency is defined by Equations (3) and (4). When the migrated voxel v_m has been received and processed by LP_{dst}, these invariants are replaced by Invariant (IV1), stating that v_m is locally consistent with all its neighbors $v \in LP_{dst}$. Again, we omit the details.

5.2.3 Consistency between voxel being migrated and neighboring voxels on other domains. Let v_m, v be two neighboring voxels, where v_m is being migrated from LP_{src} to LP_{dst} and v is located on a third LP, LP_w, as depicted in Figure 1. At the transmission of $\overrightarrow{v_m}$, a message mv_{v_m} is sent to all neighboring LPs except the receiver of $\overrightarrow{v_m}$ (line 10 in Algorithm 1). At the receipt of $\overrightarrow{v_m}$, a message recv_{v_m} is sent to all neighbors, except the sender of $\overrightarrow{v_m}$ (line 11 in Algorithm 2). Thus, in the following, we have to take into account if the control messages mv_{v_m} and recv_{v_m} have been received or not, since they affect the protocol. We split the argument into the two possible directions in which messages may be sent, viz. $v_m \to v$ and $v \to v_m$.

Case $v_m \to v$: We let $-t$ be the earliest anti-message preceding the message mv_{v_m} in $chan_{\text{src}\to w}$ or succeeding the message recv_{v_m} in $chan_{\text{dst}\to w}$. The cut operator reflects that anti-messages change in meaning upon receipt of mv_{v_m} (line 31 in algorithm 2). After the transmission of $\overrightarrow{v_m}$, but before mv_{v_m} has been received by LP_w, we have

$$\text{rm}_t(\text{In}^{v_m}(v)) +\!\!+ \underset{v_m \to v}{\text{effect}}(\text{cut}_{\text{mv}_{v_m}}(chan_{\text{src}\to w}) +\!\!+ chan_{\text{dst}\to w}) = \text{Out}^v(v_m). \tag{IV5}$$

Intuitively, this invariant extends (IV2) by considering that diffusions from v_m to v are found preceding mv_{v_m} in $chan_{\text{src}\to w}$. After the reception of v_m by LP_{dst}, they are then transmitted over $chan_{\text{dst}\to w}$. We also note, that after the reception of mv_{v_m} by LP_w, any outstanding diffusions from v_m to v are in $chan_{\text{dst}\to w}$, obeying the corresponding instance of (IV2).

Case $v \to v_m$: In this direction, we have two cases, depending on whether LP_w has yet observed the migration or not:

- mv_{v_m} has been received by LP_w.
  We let t be the time of the earliest anti-message in $chan_{w\to\text{dst}}$ following forw_{v_m}; if forw_{v_m} is not in $chan_{w\to\text{dst}}$, let t be the time of the earliest anti-message in $chan_{w\to\text{dst}}$. Then

$$\text{rm}_t(\text{In}^v(v_m)) +\!\!+ \underset{v \to v_m}{\text{effect}}(chan_{w\to\text{dst}}) = \text{Out}^v(v_m) \tag{IV6}$$

  This invariant is essentially the same as (IV2).

- mv_{v_m} has not been received by LP_w.
  We let t be the time of the earliest anti-message in $log_{w\to\text{src}}(v_m)$ and $chan_{w\to\text{src}}$.

$$\text{rm}_t(\text{In}^v(v_m)) + \underset{v\to v_m}{\text{effect}}(log_{w\to\text{src}}(v_m) + chan_{w\to\text{src}}) = \text{Out}^v(v_m) \quad \text{(IV7)}$$

  This invariant reflects that messages from v to v_m are stored in $log_{w\to\text{src}}(v_m)$ until mv_{v_m} is received by LP_w.

Invariants (IV6) and (7) are also established by induction over the steps of the algorithm. Details are omitted for space reasons.

6 LOAD BALANCING

In this section, we describe the load metric, the communication metric, and the load balancing algorithm that we use for the evaluation of the load migration protocol in the next section.

Load balancing can be seen as an online local rebalancing technique for data partitioning. In our case, the simulator is given an initial partition of the model, generated offline by the METIS library [21]. Due to factors not available to the offline partitioning, such as a dynamic or variable load, the partitions may need continuous rebalancing locally to ensure that the load remains balanced. Data partitioning and rebalancing algorithms typically try to optimize for a balanced workload and minimize communication.

For the evaluation of the migration protocol we selected a load balancing that takes two metrics into account: a load metric based on the number of rollbacks caused by stragglers received at a particular voxel, which is used to initiate a load balancing locally, and a communication minimizing step that selects some voxel in the vicinity whose migration minimizes communication. Below, we first define the metrics, and then the load balancing algorithm.

The load metric is defined per voxel. We define the *inverse voxel load* for a period of wall-clock time Δt and voxel v as

$$L_v = \frac{\Delta t}{\Delta r_v},$$

where Δr_v is the total number of rollbacks during time Δt, including secondary, that are incurred due to stragglers received at v. The measure could be seen as the mean distance, in wall clock time, between two consecutive rollbacks. The *inverse rate of rollbacks* is then defined as the limit of L_v as Δt goes to 0.

We define the communication metric, or the *gain*, of a voxel v on LP LP_i relative a neighboring LP LP_j as

$$g_{ij}(v) = \frac{||\{E(v,v') \mid v' \in \text{LP}_j\}||}{||\{E(v,v') \mid v' \in \text{LP}_i\}||},$$

where $E(v,v')$ denotes an edge, i.e., a communication channel, between v and v'. Thus, the gain is defined as the *external degree* towards LP_j over the *internal degree*. The gain as defined above describes how well connected a voxel is to its domain.

The load balancing algorithm is defined in terms of the load metric and the gain of a voxel. If the inverse rate of rollbacks surpasses a threshold, R, then a request for load balancing is sent to the LP LP_src that sent the last straggler to v (a simplification, which nevertheless should result in a correct destination of the request most of the time). Upon receipt of the request at LP_src, the voxel neighbor to v with the highest gain is selected for migration. To limit bad migrations that do not improve the load or communication balance, we introduce a *gain threshold*, G, so that only voxels with a gain superior to G may be migrated.

The successful migration of one or more of the neighboring voxels to v, based on the load and communication metrics defined above, would serve two purposes. First, migrating voxels balances the amount of work between two LPs, and potentially reduces the number of future rollbacks. Second, a high rate of rollbacks at the boundary also means a high rate of local communication between two or more voxels located on different LPs. The migration thus also reduces inter-LP communication, if the voxels to migrate are chosen wisely, e.g., by selecting to migrate the voxel that minimizes the communication.

7 EVALUATION

In this section, we evaluate the performance of the migration protocol coupled with the load balancing algorithm and the load and communication metrics defined in Section 6. We try to specifically understand the performance of the migration protocol and its shortcomings, as it can be used together with many different load balancing algorithms and load and communication metrics.

We look at the following questions:

- What is the overhead of the migration protocol? (Section 7.4)
- How to tune the threshold for the load measure? (Section 7.5)
- How well does the protocol, together with a load balancing algorithm, adapt to a changing load? (Section 7.6)
- How does load balancing perform compared to optimism control? (Section 7.7)

7.1 Algorithms Evaluated

For the evaluation of the load balancing algorithm, we use three algorithms:

NSM An efficient sequential NSM implementation, taken from the URDME framework[11].

R-PNSM The so-called Refined PNSM algorithm of [24], that uses optimism control.

PNSM-LB The load balancing parallel NSM algorithm described in this paper, derived from the R-PNSM algorithm.

We compare the results of the PNSM-LB algorithm with and without load balancing activated to the sequential NSM algorithm and the parallel R-PNSM algorithm. Of particular interest is that the R-PNSM algorithm include optimizations that are possible when statically assigning the partitions to LPs. One such optimization is that there is only a single rollback history per LP. In contrast, the load balancing parallel NSM algorithm of this paper has arranged the data so that each voxel easily can be moved from one LP to another; in particular, each voxel has its own rollback history. We can estimate the cost of the compromises that we have taken when restructuring the parallel NSM algorithm to enable load migration, by comparing the performance of the PNSM-LB algorithm without load balancing to the performance of the R-PNSM algorithm.

7.2 Benchmarks

To evaluate the algorithm, we use two types of benchmarks:

- Simulation of the Min-protein system in a three-dimensional unstructured (i.e., an irregular mesh) model of the *E. coli*

bacterium [14]. The Min-protein has a central role in the cell division of the bacterium, where the oscillation of the min-proteins help determine the position of the septum, the new cell wall. The model consists of 5 species, and the dynamics are described by 5 reactions. It is complicated by some reactions only taking place on the membrane of the cell. We present data for two different stages of cell division, short and long, comprising 1500 and 2700 voxels, respectively. The two models are denoted mincde[s] and mincde[l], respectively. Due to the oscillation of the proteins, the load is highly dynamic. Since the number of voxels is small, the amount of available parallelism is limited.

- Simulation of a reversible isomerization process, where two species are randomly transformed into each other, and may diffuse freely with equal diffusion rates within a spherical domain. The domain is represented as a 3-dimensional unstructured mesh, and comprises ~ 13000 voxels. The load is well balanced, and the number of reaction events stand in a 1:10 proportion to the number of diffusions events. The model is denoted sphere.

7.3 Experimental Setup

The experiments are run on a 4 socket Intel Sandy Bridge E5–4650 machine. Each processor has 8 cores and 20 MB L3-cache. Hyper-threading was turned off, and threads were pinned to cores. The operating system of the machine is Linux 4.9.0, and the binaries were compiled using GCC version 6.3.0. The models were initially partitioned using the multilevel k-way partitioning method from the METIS library [21].

7.4 Overhead of Migration Protocol

We would like to understand how much overhead the migration protocol incurs during a simulation. The migration of a voxel may cause rollbacks, which in turn may cause anti-messages. Therefore, we have traced the time spent sending and receiving all types of control messages involved in a migration, including time spent on processing rollbacks and anti-messages generated by the migration of a voxel. In none of the benchmark runs presented here did the total cost of the migration protocol exceed 0.5%.

7.5 Tuning of the Rate and Gain Parameters

In this section, we tune the inverse rollback rate parameter R for locally initiating a migration of a voxel and the gain threshold parameter G, as described in Section 6.

In Figures 2 and 3, results for tuning of the inverse rollback rate parameter R and the gain threshold parameter G of the migration mechanisms is presented. In the figures, each line represents one value of the gain threshold. R is varied from 0 (no migration) to 80, and the gain threshold is varied from 0.5 to 0.7. The left hand sub-figure within each figure shows the speedup relative to not using migration, and the right hand sub-figure shows the total number of rollbacks occurring during the simulation. In Figure 2 the tuning is done on the mincde[s] benchmark for 3 threads. The maximum speedup, of about 15% over when no migration is used, is reached with a rollback rate threshold R of 40, and a gain threshold G of 0.6–0.7. In Figure 3, the tuning is done on the same benchmark, run

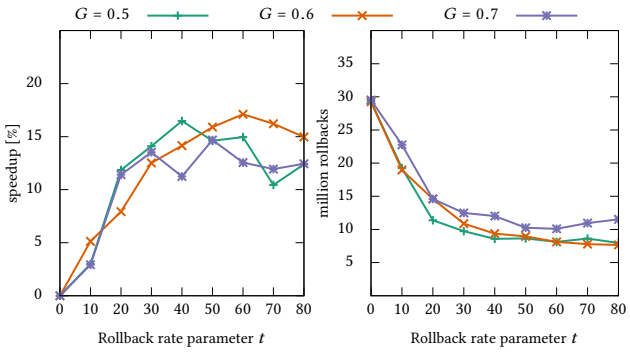

Figure 2: Inverse rollback rate parameter R impact on the number of rollbacks and speedup. Evaluated on the mincde[s] **benchmark, 3 threads. Speedup relative $R = 0$.**

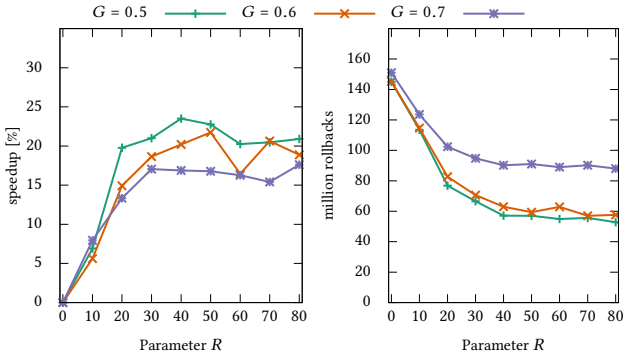

Figure 3: Inverse rollback rate parameter R impact on the number of rollbacks and speedup. Evaluated on the mincde[s] **benchmark, 16 threads. Speedup relative $R = 0$.**

with 16 threads. Here, the maximum speedup, with an improvement of 25% over when no migration is used, is reached at a rollback rate threshold R of 10–20, for a gain threshold G of 0.6–0.7. Beyond $R = 20$, the results tend to become noisier, not resulting in significantly better speedup than for a low rollback rate threshold.

In general, the run time improvement of using load migration over not using migration peaks at about 25%, with greater improvement being achieved for more threads. With a few number of threads, each thread has more work to do, and thus leaving less room for improvement by load balancing. The number of rollbacks is greatly reduced, by a factor of 2–4. The decrease in rollbacks is in line with the performance improvement, given the amount of time spent on rollbacks relative the total execution time.

7.6 Effective Utilization

In this section, we look at the effect load balancing has on the amount of time individual LPs spend on rollback overhead, i.e., processing rollbacks and redoing the rolled back time interval (roughly estimated to take the same amount of time as the rollbacks themselves) and anti-messages, denoted *non-useful* work. In Figure 4, we visualize a simulation run of the mincde[s] benchmark on 16 threads. Each bar represents the time allocation of one individual

LP, divided into useful and non-useful work. The variance of the amount of time spent on non-useful work is more than halved when using migration. However, as can be seen by the amount of non-useful work even with load balancing activated, we can conclude that the load imbalance is still momentarily high during the simulation.

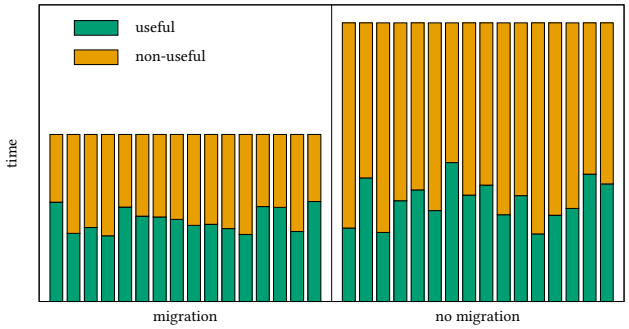

Figure 4: Instrumentation data for each thread of the R-PNSM and PNSM-LB algorithms on the mincde[s] **benchmark, 16 threads.**

To illustrate in more detail, we try to visualize the rollbacks and the behavior of the load balancing mechanism during a simulation. In Figures 5 and 6, a timeline of the simulation of the mincde[s] benchmark with the PNSM-LB algorithm on 3 threads is depicted. For each thread, one individual timeline is depicted, horizontally. In each timeline, the total population, the number of voxels, and the number of rollbacks is shown. In Figure 5, no migration is used. We see how the population varies with time, and how the number of rollbacks increases when the population difference between LPs is big. We also see how the middle LP always has more work to do than its two neighbors, and suffers from practically no rollbacks. In Figure 6, migration is used. We see that during the entire simulation, there are much fewer rollbacks, and the rollbacks are more evenly distributed over the LPs. The population still varies, but the middle LP has in general a lower population than in Figure 5, i.e., the load is better balanced.

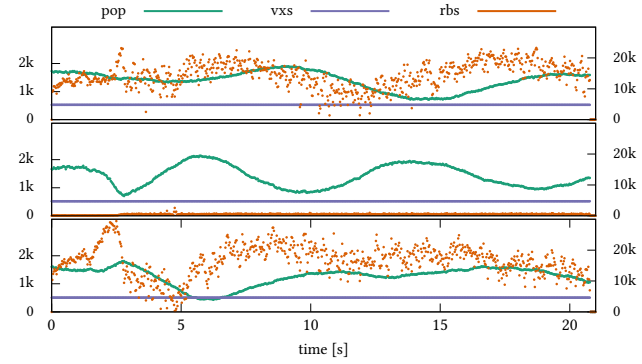

Figure 5: Time series of the population, number of voxels and rollbacks per LP in the mincde[s] **benchmark run with the PNSM-LB algorithm without load balancing for 3 threads.**

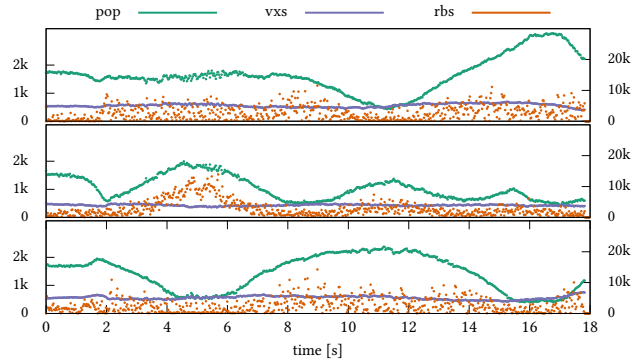

Figure 6: Time series of the population, number of voxels and rollbacks per LP in the mincde[s] **benchmark run with the PNSM-LB algorithm with load balancing for 3 threads.**

7.7 Performance

In this section, we compare the scaling of the PNSM-LB algorithm with and without load migration, and also compare it to the R-PNSM algorithm, from which it is derived.

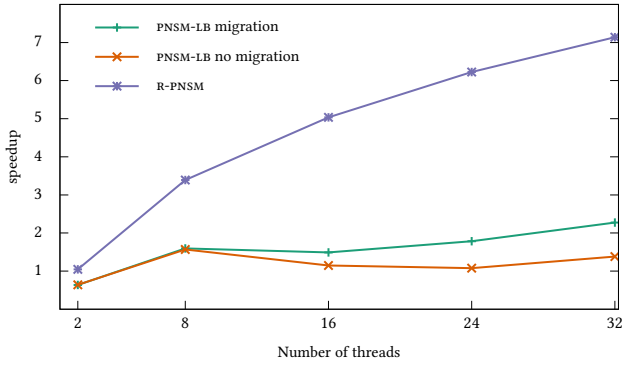

Figure 7: scaling over NSM on the sphere[s] **benchmark.**

First, in Figure 7, we see the speedup over the sequential NSM for the parallel algorithms, evaluated on the sphere[s] benchmark. The benchmark is uniform in load, and we see as expected that the R-PNSM algorithm, which does not have any control logic to handle migrations, perform much better. However, for the PNSM-LB algorithm, that has been restructured to handle migrations, using load balancing is better than not using load balancing, with up to a 65% better speedup on 32 threads. The fact that there actually is an improvement indicates that the initial partitioning provided by the METIS library is not perfect. In Figures 8a and 8b, we see the speedup over NSM for the parallel algorithms, evaluated on the mincde[s] and the mincde[l] benchmarks, respectively. We see that for up to 8 threads, the parallel algorithms show approximately the same performance. For 16 threads, the R-PNSM algorithm clearly has better performance. The difference between the PNSM-LB algorithm with and without load balancing is minimal for less than 16 threads. We believe this to be due to a suboptimal load balancing algorithm, that does not make the best decision on where to move and when to move the voxels. For 16 threads, using load balancing results in

approx. 25% better speedup than when not using load balancing, in both benchmarks.

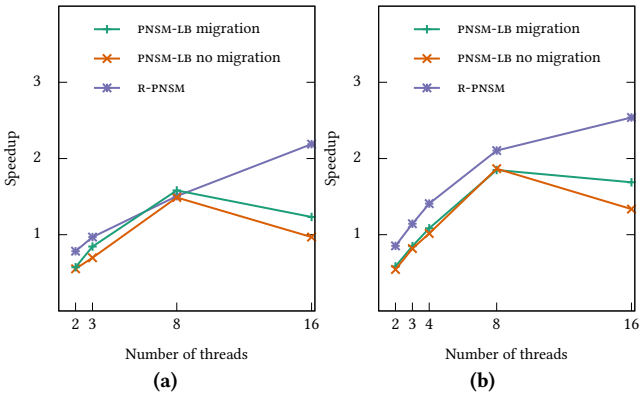

Figure 8: Scaling over NSM on the mincde[s] **(a) and the** mincde[l] **(b) benchmarks.**

In general, we see that the R-PNSM algorithm scales better than the PNSM-LB algorithm, particularly for the benchmark with the well-balanced model (Figure 7). We note again that the PNSM-LB algorithm is derived from the R-PNSM algorithm. Hence, the difference in scalability between the R-PNSM algorithm and the PNSM-LB algorithm without load balancing represents the performance cost of modifying the algorithm so that load balancing can be applied. E.g., intra-LP diffusions, which make up the majority of the events, affect two voxels, and require updating one event history per affected voxel in the PNSM-LB algorithm, instead of a single event history as in the R-PNSM algorithm.

8 CONCLUSIONS

We have described a load migration protocol aimed at fine-grained dynamic load balancing. The protocol works across aggregated anti-messages, a technique used to reduce inter-LP communication. The protocol has been evaluated together with a local load metric and load balancing algorithm. The load balancing is shown to reduce the number of incurred rollbacks by a factor of 2–4, and the speedup is improved by up to 25%, due to a reduced number of rollbacks.

We observe that the main challenge is the performance penalty incurred by restructuring the existing PDES algorithm in such a way that it is suitable for load balancing. We hypothesize that the R-PNSM algorithm benefits from having better data locality and more efficiently uses shared data structures, such as the event history and the model state.

ACKNOWLEDGMENTS

This work was supported in part by the Swedish Research Council within the UPMARC Linnaeus centre of Excellence.

We would like to thank the reviewers for their observant and helpful comments.

REFERENCES

[1] H. Avril and C. Tropper. 1996. The Dynamic Load Balancing of Clustered Time Warp for Logic Simulation. *SIGSIM Simul. Dig.* 26, 1 (July 1996), 20–27.
[2] P. Bauer, J. Lindén, S. Engblom, and B. Jonsson. 2015. Efficient Inter-Process Synchronization for Parallel Discrete Event Simulation on Multicores. In *Proc. SIGSIM PADS*. ACM, 183–194.
[3] A. Boukerche and S. K. Das. 1997. Dynamic load balancing strategies for conservative parallel simulations. *SIGSIM Simul. Dig.* 27, 1 (June 1997), 20–28.
[4] C. Burdorf and J. Marti. 1993. Load Balancing Strategies for Time Warp on Multi-User Workstations. *Comput. J.* 36, 2 (1993), 168–176.
[5] C. D. Carothers and R. M. Fujimoto. 1996. Background Execution of Time Warp Programs. *SIGSIM Simul. Dig.* 26, 1 (July 1996), 12–19.
[6] L. Chen, Y. Lu, Y. Yao, S. Peng, and L. Wu. 2011. A Well-Balanced Time Warp System on Multi-Core Environments. In *Proc. PADS*. IEEE, 1–9.
[7] M. Choe and C. Tropper. 1999. On learning algorithms and balancing loads in Time Warp. *Proc. PADS*, 101–108.
[8] S. R. Das. 2000. Adaptive Protocols for Parallel Discrete Event Simulation. *J. Oper. Res. Soc.* 51, 4 (2000), 385–394.
[9] E. Deelman and B. K. Szymanski. 1997. Breadth-First Rollback in Spatially Explicit Simulations. In *Proc. PADS*. IEEE, 124–131.
[10] E. Deelman and B. K. Szymanski. 1998. Dynamic Load Balancing in Parallel Discrete Event Simulation for Spatially Explicit Problems. *SIGSIM Simul. Dig.* 28, 1 (July 1998), 46–53.
[11] B. Drawert, S. Engblom, and A. Hellander. 2012. URDME: a modular framework for stochastic simulation of reaction-transport processes in complex geometries. *BMC Syst. Biol.* 6, 76 (2012).
[12] K. El-Khatib and C. Tropper. 1999. On Metrics for the Dynamic Load Balancing of Optimistic Simulations. In *Proc. Hawaii Int'l Conf. on System Sciences*. IEEE.
[13] J. Elf and M. Ehrenberg. 2004. Spontaneous separation of bi-stable biochemical systems into spatial domains of opposite phases. *Syst. Biol.* 1, 2 (2004), 230–236.
[14] D. Fange and J. Elf. 2006. Noise-Induced Min Phenotypes in E. coli. *PLOS Comput. Biol.* 2, 6 (June 2006), e80.
[15] R. M. Fujimoto. 1990. Parallel Discrete Event Simulation. *Commun. ACM.* 33, 10 (1990), 30–53.
[16] B. P. Gan, Y. H. Low, S. Jain, S. J. Turner, W. Cai, W. J. Hsu, and S. Y. Huang. 2000. Load Balancing for Conservative Simulation on Shared Memory Multiprocessor Systems. In *Proc. PADS*. IEEE, 139–146.
[17] C. W. Gardiner. 2007. *Handbook of stochastic methods*. Springer.
[18] D. W. Glazer and C. Tropper. 1993. On Process Migration and Load Balancing in Time Warp. *IEEE Trans. Parallel Distrib. Syst.* 4, 3 (1993), 318–327.
[19] S. Jafer, Q. Liu, and G.A. Wainer. 2013. Synchronization methods in parallel and distributed discrete-event simulation. *Simul. Model. Pract. Th.* 30 (2013), 54–73.
[20] D. R. Jefferson. 1985. Virtual Time. *ACM Trans. Program. Lang. Syst.* 7, 3 (1985), 404–425.
[21] G. Karypis and V. Kumar. 1998. A Fast and High Quality Multilevel Scheme for Partitioning Irregular Graphs. *SIAM J. Sci. Comput.* 20, 1 (Jan. 1998), 359–392.
[22] J. I. Leivent and R. J. Watro. 1993. Mathematical Foundations of Time Warp Systems. *ACM Trans. Program. Lang. Syst.* 15, 5 (1993), 771–794.
[23] Z. Lin and Y. Yao. 2015. Load Balancing for Parallel Discrete Event Simulation of Stochastic Reaction and Diffusion. In *Int'l Conference on Smart City/SocialCom/SustainCom*. IEEE, 609–614.
[24] J. Lindén, P. Bauer, S. Engblom, and B. Jonsson. 2017. Exposing Inter-Process Information for Efficient Parallel Discrete Event Simulation of Spatial Stochastic Systems. In *Proc. SIGSIM PADS*. ACM, 53–64.
[25] J. Misra. 1986. Distributed Discrete-Event Simulation. *ACM Comput. Surv.* 18, 1 (1986), 39–65.
[26] A. Pellegrini, R. Vitali, S. Peluso, and F. Quaglia. 2012. Transparent and Efficient Shared-State Management for Optimistic Simulations on Multi-core Machines. In *Proc. MASCOTS*. IEEE, 134–141.
[27] P. Peschlow, T. Honecker, and P. Martini. 2007. A Flexible Dynamic Partitioning Algorithm for Optimistic Distributed Simulation. In *Proc. PADS*. IEEE, 219–228.
[28] P. L. Reiher and D. R. Jefferson. 1990. Virtual Time Based Dynamic Load Management in the Time Warp Operating System. *Trans. Soc. Comput. Simul. Int.* 7, 9 (1990), 103–111.
[29] F. Sarkar and S. K. Das. 1997. Design and implementation of dynamic load balancing algorithms for rollback reduction in optimistic PDES. In *Proc. MASCOTS*. IEEE, 26–31.
[30] R. Schlagenhaft, M. Ruhwandl, C. Sporrer, and H. Bauer. 1995. Dynamic Load Balancing of a Multi-cluster Simulator on a Network of Workstations. *SIGSIM Simul. Dig.* 25, 1 (July 1995), 175–180.
[31] J. Wang, D. Jagtap, N. B. Abu-Ghazaleh, and D. Ponomarev. 2014. Parallel Discrete Event Simulation for Multi-Core Systems: Analysis and Optimization. *IEEE Trans. Par. Distr. Syst.* 25, 6 (2014), 1574–1584.
[32] L. F. Wilson and W. Shen. 1998. Experiments in Load Migration and Dynamic Load Balancing in SPEEDES. In *Proc. 30th Winter Simulation Conf.* IEEE, 483–490.
[33] Y. Xu, W. Cai, D. Eckhoff, S. Nair, and A. Knoll. 2017. A Graph Partitioning Algorithm for Parallel Agent-Based Road Traffic Simulation. In *Proc. SIGSIM PADS*. ACM, 209–219.